*Article*

# Evaluation of the Effect of Ethanol on the Properties of Acrylic-Urethane Samples Processed by Vat Photopolymerization

Dorota Tomczak [1], Wiesław Kuczko [2], Ariadna B. Nowicka [3], Tomasz Osmałek [4], Mirosław Szybowicz [3], Monika Wojtyłko [4] and Radosław Wichniarek [2,*]

[1]  Institute of Chemical Technology and Engineering, Poznan University of Technology, Berdychowo 4, 60-965 Poznan, Poland; dorota.tomczak@doctorate.put.poznan.pl
[2]  Faculty of Mechanical Engineering, Poznan University of Technology, Piotrowo 3, 61-138 Poznan, Poland
[3]  Faculty of Materials Engineering and Technical Physics, Poznan University of Technology, Piotrowo 3, 60-965 Poznan, Poland
[4]  Chair and Department of Pharmaceutical Technology, Poznan University of Medical Sciences, Rokietnicka 3, 60-806 Poznan, Poland
*  Correspondence: radoslaw.wichniarek@put.poznan.pl

**Abstract:** The aim of the study was to investigate the effect of ethanol on the properties of acrylic-urethane resin products obtained by vat photopolymerization using the masked stereolithography method. The effect of alcohol at concentrations of 15, 25, and 35% in the resin on the chemical structure, weight, thickness of the samples, and mechanical properties in static tabltensile tests performed immediately after printing and one month later were studied. The results obtained were evaluated in terms of the use of ethanol as a cosolvent to help load the resin with agomelatine for the potential of obtaining microneedle transdermal systems. It was shown that in terms of stability of properties, the most favorable system was resin with the addition of alcohol at a concentration of 15%. The greatest changes induced by the presence of the solvent in the resin were observed in the case of tensile properties, where the alcohol caused a decrease in the plasticity of the material, reducing the relative elongation at break from 14% for the pure resin to 4% when the alcohol concentration was 35%. Young's modulus and tensile strength also decreased with the addition of alcohol by 18% and 31%, respectively, for testable samples with the maximum amount of alcohol in the resin. The deterioration in properties is most likely related to the effect of the solvent on the radical polymerization process of the resin, particularly the phenomenon of chain transfer to the solvent, which is important in view of the intended application of the developed material.

**Keywords:** masked stereolithography; vat photopolymerization; acrylic-urethane resin; radical polymerization; solvent

## 1. Introduction

The ability to customize products for a given application, especially the personalization of medical and pharmaceutical devices such as drugs, prostheses, tools, and implants, and the possibility of prototyping and the speed of obtaining components, as well as the very low level of waste produced during the process are among the many advantages of the additive manufacturing methods currently being developed [1]. In this group of methods, components are built up layer by layer, using different techniques to solidify the material. Various materials can be used for this purpose, but of particular note are polymeric materials, which are widely used in many industries due to their properties. The additive manufacturing methods that use plastics as the source material are material extrusion, vat photopolymerization, sheet lamination, and material jetting [1–3]. The resin techniques included in vat photopolymerization, such as stereolithography (SLA), digital light processing (DLP), or multiJet printing (MJP), are based on the use of photocurable resins [4]. Using the aforementioned techniques, it is possible to obtain products with

complex geometries and very high dimensional accuracy, especially when compared to the capabilities of the most popular polymer processing additive manufacturing method—fused filament fabrication [5].

One technique that stands out from the aforementioned vat photopolymerization is DLP, which, thanks to the use of a digital mirror device (DMD), allows exposure and simultaneous curing of the entire layer of the printed part, making the process faster but still very accurate. Masked stereolithography (MSLA) is another method that also allows full-layer exposure, but is easier to implement and, therefore, more accessible to a wider user base. To obtain parts by MSLA or DLP, photocurable resins are used, most often characterized by UV-activated radical polymerization [6]. The components of the resin are mainly acrylic oligomers and mers, a photoinitiator and additives in the form of a co-initiator, inert dyes, and photosensitizers [7]. During exposure to radiation, free radicals are formed from the photoinitiator, which, thanks to the functional groups present in the mers and oligomers, lead to cross-linking of the polymer structure. The design of a suitable package of images given to the DMD, corresponding to individual layers of the manufactured samples, makes it possible to obtain samples with dimensions on the order of micrometers [8].

A promising application of the MSLA technique is the manufacture of microneedle transdermal systems (MTSs). These are devices designed to create microchannels in the human skin that allow drug delivery and increase bioavailability. There are five main types of microneedles: solid, hollow, dissolving, coated, and hydrogel [9,10]. An essential aspect of each type of microneedle is its geometry and dimensional accuracy, which must be maintained over time. Conventional injections can cause pain, but MTSs, with lengths that penetrate the stratum corneum without irritating nociceptors, offer a less painful alternative while maintaining mechanical strength. MSLA and DLP can produce various microneedles, particularly hydrogel drug-loaded systems that swell in the presence of a medium like water from human skin, allowing drug diffusion [11].

To manufacture such systems, the active ingredient must be mixed into the matrix material before the MTS fabrication or attached to the microneedles [11]. The potential of MSLA and DLP is enhanced by the ability to mix additives into photocurable resins that behave like hydrogels [12]. Previous research has explored various composites with a photocurable resin matrix, including acrylates with hollow glass microspheres [13] or a matrix of acrylated epoxidized soybean oil and carbon nanotubes [14]. Resin-based composites are also used in the production of ceramic or metallic sinters by a UV-exposing resin mixed with inorganic particles [15,16]. In the pharmaceutical field, resins loaded with drugs such as 5-fluorouracil [17] or biocompatible resins with acetyl-hexapeptide-3 [18] have been developed for biomedical applications, including transdermal systems.

For certain substances and fillers, additional agents are required to disperse or dissolve the filler, especially when the particles aggregate easily or differ in physicochemical properties from the matrix material. Acetone or ethanol can be used for this purpose [14,15,19]. However, solvents, cosolvents, and dispersion aids significantly impact the properties of the final products by affecting the resin polymerization process, particularly radical polymerization [20]. Evaporating the solvent can reduce its impact but introduces additional procedures that increase energy consumption and costs. Moreover, distillation may evaporate other resin components with similar vapor pressures, which is undesirable.

Agomelatine, an antidepressant drug, requires a cosolvent for mixing into acrylic resin. Although it is lipophilic, it is difficult to dissolve directly in a resin without a cosolvent. The oral administration of agomelatine affects the gastrointestinal tract, including the liver, and is limited by the first-pass effect, reducing its bioavailability, which transdermal administration can bypass [21]. Therefore, this study investigates how ethanol, a cosolvent for dissolving agomelatine and other lipophilic substances in a resin, affects the properties of the products, including mechanical strength, dimensional stability, and mass stability. The research aims to determine the maximum alcohol content that maintains the desired

properties of the final products, thus establishing the maximum amount of agomelatine for potential microneedle transdermal systems.

## 2. Materials and Methods

### 2.1. Materials

As part of the conducted research, a biocompatible resin based on low molecular weight urethane acrylate polymer with the trade name Raydent SG (Esdent, Wroclaw, Poland) was used to obtain samples. Resin biocompatibility is Class I by Rule 5 of Annex IX, MDD 93/42/EEC as amended by Directive 2007/47/EC of the European Parliament. In addition to acrylic-urethane polymers, the resin contains other organic substances, including the photoinitiator 2,4,6-trimethylbenzoyl-diphenyl phosphine oxide (DPPO) and 4-methoxyphenol [22]. Additionally, 96% ethanol (Avantor Performance Materials, Gliwice, Poland) was used as the solvent.

### 2.2. Sample Preparation

In the production of experimental samples, the Phrozen Sonic Mini 8K (Phrozen Tech, Hsinchu city, Taiwan) device was used. This device operates according to the MSLA method. Samples were obtained from pure resin and from resin to which alcohol was added so that the concentrations were 15, 25, and 35% *w/w*. The process of obtaining samples with a given alcohol concentration was as follows: A solution of 20 g of resin and the appropriate amount of alcohol was prepared, the ready solution was poured into a vat, then 5 rectangular samples of $80 \times 10 \times 2$ mm were printed simultaneously, arranged with the largest surface adjacent to the table at a distance of 2.5 mm from each other. The samples were exposed for 10 seconds for the first eight bottom layers and 3 seconds for the other layers. The layer thickness was 0.05 mm and the transition layer count was 0. The retract distance and speed were 5 mm and 10 mm/s, respectively. The rest time after retraction was 5 s. After printing, the samples were pulled off the table and washed in isopropyl alcohol for 2 min and then cured for 10 min in a UV Curing Chamber machine (XYZPrinting, New Taipei, Taiwan). The remaining resin in the vat was poured, and the vat was cleaned. The whole described operation was performed 4 times for each concentration of alcohol and pure resin, obtaining 4 series in each process.

### 2.3. Tensile Testing

Static tensile tests were conducted at a rate of 1 mm/min to obtain characteristic parameters such as modulus of elasticity, tensile strength, and relative strain. All measurements were performed at room temperature using a Zwick/Roell Z020 testing machine (Zwick Roell, Ulm, Germany) in accordance with ISO 527 standards.

### 2.4. Geometry and Mass Measurements

To verify the change in the geometry of the products, the thickness of the samples (nominal 2 mm) was measured immediately after manufacture and one month later. The measurements were carried out using a Baker thickness gauge type J 130/7 (Baker, Pune, India). Similarly, the weight of the samples was measured using a Radwag AS 220.X2 laboratory balance (Radwag, Radom, Poland).

### 2.5. Raman Spectroscopy Measurements

The nonpolarized Raman spectra were recorded in the backscattering geometry using a Renishaw inVia micro-Raman system (Wotton-under-Edge, Gloucestershire, UK). An infrared solid-state laser operating at λ = 785 nm was used as the source of excitation light, with a power of less than 20 mW. The incident laser beam was tightly focused on the sample surface through a Leica $50\times$ LWD (long working distance) microscope objective. Five spectra were collected for each sample in the range of 200 to 3200 $\text{cm}^{-1}$, with a spectral resolution of 2 $\text{cm}^{-1}$. Then, the average spectrum was calculated based on these five origin

spectra, followed by additional calculations. All measurements were performed in air at room temperature two months after curing.

## 3. Results and Discussion

### 3.1. Obtained Samples

The samples were obtained according to the process described in the methodology. The reason for each replacement of the resin solution with alcohol with a fresh one and keeping the processing parameters constant was to ensure the stability of the manufacturing conditions so that the effect of changing only one factor, the alcohol concentration, could be effectively evaluated. Samples made from pure resin were transparent, while white discoloration appeared on samples with alcohol added at a concentration of 15%. There was more and more discoloration with increasing alcohol content, until for an alcohol concentration of 35%, the samples obtained were entirely white. The described phenomenon is shown in Figure 1. Attempts to add 45% alcohol failed due to insufficient adhesion of the cured bottom layers to the table, causing sample detachment during printing.
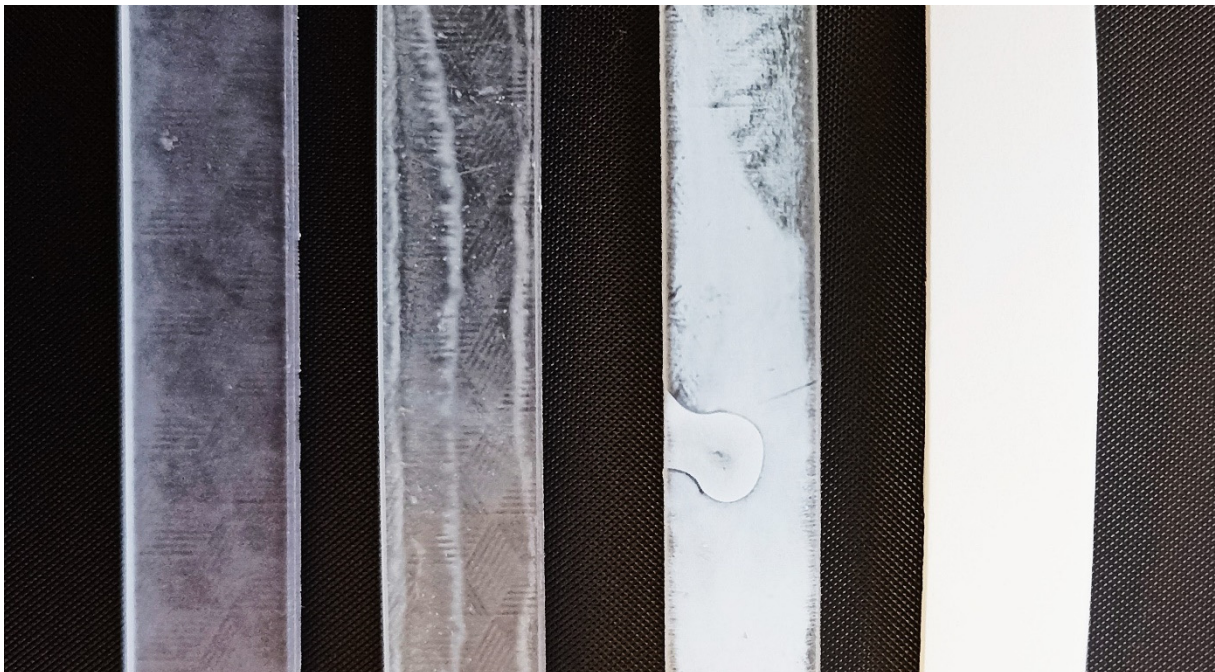


**Figure 1.** Photo of representative samples made from (from the left): resin, and resin with an alcohol content of 15%, 25%, and 35%.

### 3.2. Mass and Geometry Analysis

The average thickness and weight values given with the standard deviation and spread of the data measured immediately after printing (denoted as 0 mth) and one month after printing (denoted as 1 mth) for samples made of pure resin (denoted as resin) and with 15, 25, and 35% alcohol (denoted by the corresponding ethanol percentage) are given in Tables 1 and 2, respectively. The samples were kept at room temperature, with an average air humidity of approximately 40%, and without exposure to excessive sunlight. The average thickness for the samples made with resin was 2.09 mm, deviating from the nominal dimension by 0.09 mm. In [23], a similar phenomenon of deviation of the dimensions of the samples from the nominal dimension by a value of about 0.1 mm was observed using the same printer and the same type of calibration. Therefore, it can be concluded that this phenomenon depends not on the resin used but on the device used and its preparation, including the established parameters and calibration. As the alcohol concentration in the resin increased, the average sample thickness increased from an initial

value of 2.09 to 2.13 mm, but with a decreasing standard deviation value from 0.03 for pure resin samples to 0.01 mm for samples with 35% alcohol content. It can be said that the thickness values for all samples were comparable but the pure resin samples had the least dimensional stability. Confirmation is also provided by the data range, which for samples made of pure resin, was 0.12 mm, and for samples with 35% alcohol content, was less than half this. After one month, the average thickness of the sample made of pure resin decreased by 0.02 mm; similarly, the range decreased from 0.12 to 0.05 mm. For samples with alcohol added, the average thickness after one month was also smaller. The more alcohol added, the greater the difference in average thickness of the samples measured immediately after manufacture and one month later, being as much as 0.14 mm for a concentration of 25% with a data range of 0.11 mm. For samples with a concentration of 35%, the thickness results after one month are not given due to the significant deformation (bending along the largest overall dimension) of the samples over time, making it impossible to measure the thickness with the chosen technique.

**Table 1.** Average thickness of samples and values range measured right after manufacturing (0 mth) and 1 month later (1 mth).

|  |  | **Resin** | **15%** | **25%** | **35%** |
|---|---|---|---|---|---|
| 0 mth | average thickness $\pm$ standard deviation (mm) | 2.09 $\pm$ 0.03 | 2.10 $\pm$ 0.02 | 2.13 $\pm$ 0.01 | 2.13 $\pm$ 0.01 |
|  | range (mm) | 0.12 | 0.09 | 0.06 | 0.05 |
| 1 mth | average thickness $\pm$ standard deviation (mm) | 2.07 $\pm$ 0.02 | 2.05 $\pm$ 0.01 | 1.99 $\pm$ 0.02 | - |
|  | range (mm) | 0.05 | 0.06 | 0.11 | - |

**Table 2.** Average mass of samples and values range measured right after manufacturing (0 mth) and 1 month later (1 mth).

|  |  | **Resin** | **15%** | **25%** | **35%** |
|---|---|---|---|---|---|
| 0 mth | average mass $\pm$ standard deviation (g) | 2.04 $\pm$ 0.03 | 1.97 $\pm$ 0.02 | 1.85 $\pm$ 0.02 | 1.50 $\pm$ 0.03 |
|  | range (g) | 0.11 | 0.08 | 0.08 | 0.09 |
| 1 mth | average mass $\pm$ standard deviation (g) | 1.87 $\pm$ 0.04 | 1.82 $\pm$ 0.01 | 1.63 $\pm$ 0.01 | 1.34 $\pm$ 0.01 |
|  | range (g) | 0.11 | 0.05 | 0.03 | 0.02 |

The average resin sample mass was 2.04 g and decreased with the addition of alcohol. Initially, at an alcohol concentration of 15%, it decreased by 0.07 g, then, when increasing the alcohol concentration to 25%, the weight decreased by 0.12, and for a concentration of 35%, the weight decreased by 0.35 g, finally reaching 1.50 g. After one month, the weight of the samples decreased by an average of 0.18 g. For the pure resin samples, the data range remained constant after a month, while for the samples with alcohol, the range decreased and was smallest for the samples with maximum alcohol content, being equal to 0.2 g.

The change in dimensions of the samples over time is most likely related to polymerization and the decrease in intermolecular spaces due to the formation of bonds within and between polymer chains (cross-links) [24]. Moreover, the addition of solvent reduces the viscosity of the solution, facilitating the migration of particles and their reaction at the initial stage of polymerization, thus increasing the effect of polymerization shrinkage due to the reduced molecular weight of polymer chains [25].

The decrease in weight of the samples with the addition of alcohol was related to the density of the ethanol, which at 0.789 g/mL, is less than that of the resin, which is about 1.1 g/mL for acrylic-urethane resins. Conversely, the change in mass over time was probably determined by the absorption of the isopropyl alcohol used to wash the samples

and its subsequent evaporation. The phenomena described may also have affected the reduction in the dimensions of the samples after one month.

### 3.3. Analysis of Mechanical Properties

The mechanical properties of the samples, specifically, Young's modulus, tensile strength, and elongation at break, are shown in Figure 2.
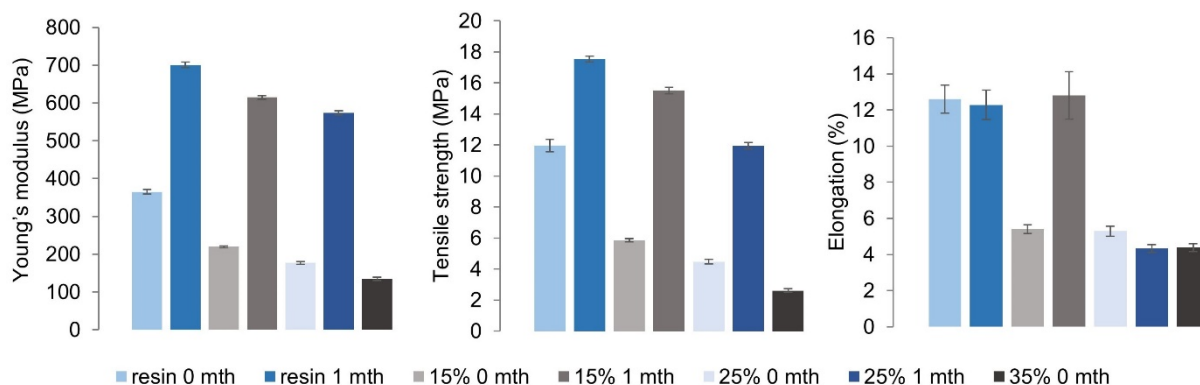


**Figure 2.** Mechanical properties of samples related to solvent amount and time of measurement.

The average value of Young's modulus for the resin samples immediately after printing is 365 MPa and almost doubles to a value of 701 MPa after one month. The addition of solvent causes a decrease in the modulus, which reaches a minimum value of 135 MPa for samples made from a resin–35% alcohol solution measured immediately after manufacturing the samples. After one month, the samples showed a significant increase in modulus compared to the values obtained for the samples immediately after printing, but with a trend of decreasing values with increasing alcohol concentration. No results were given for specimens with an alcohol concentration of 35% after one month due to their too-extensive deformation preventing the specimens from being placed without destruction in the jaws of the testing machine. Almost the same characteristics of changes in values can be seen for tensile strength, where the maximum strength value of 18 MPa was obtained with pure resin samples after one month and the minimum strength value of 3 MPa was characterized by samples with the highest alcohol concentration of 35% tested immediately after receipt. In the case of relative elongation at break, it can be observed that the elongation for the pure resin samples was almost unchanged over time at about 13%, while the addition of alcohol at a concentration of 15% reduced the elongation to 5%, which increased to about 13% after one month. For the samples with 25 and 35% alcohol, the elongation was 4–5% and did not increase after one month to a value comparable to the elongation of the pure resin samples, in contrast to the samples with 15% alcohol.

Figure 3 shows the course of the representative curves obtained during the static tensile testing of the samples. It can be seen that the resin and resin–15% alcohol samples show plastic flow after one month without a clear yield point. The other samples show mainly elastic properties before tensile rupture of the material.

The reasons for the described changes in the strength parameters of the samples can be found in the effect of the solvent on the radical polymerization process of the resin. The phenomenon is known; transferring a polymer chain to a solvent, including alcohol solvent, by abstracting the solvent atom and deactivation of the active center of the macroradical, forms a polymer chain of lower molecular weight than in the case of polymerization without solvent [26]. In the case of ethanol used as a solvent, the radicals were most likely formed by detaching a hydrogen atom from the secondary carbon atom carrying the hydroxyl group [27] due to the higher O-H bond energy of the hydroxyl group (BDE of approximately 437. 6 kJ/mol$^{-1}$) and C-H in the methyl group (BDE approximately 410.0 kJ/mol$^{-1}$) than the C-H bond energy for the carbon carrying the hydroxyl group (BDE approximately 396.6 kJ/mol$^{-1}$) [28–30]. The obtained radicals, due to the lack of steric hindrances, are

more unstable and reactive than radicals formed from resin components, which are particles that are more extended and have functional groups or branching. The introduction of particles that form highly reactive radicals into the radical polymerization process can result in an acceleration of the kinetics of the process while leading to the formation of lower molecular weight network fragments. Lower molecular weight, meanwhile, affects mechanical properties by decreasing Young's modulus and mechanical strength, which is the case with the alcohol-resin samples. Furthermore, solvent addition can reduce the formation of cross-links by attaching alcohol molecules to the cross-linker, also deteriorating the strength properties [31].
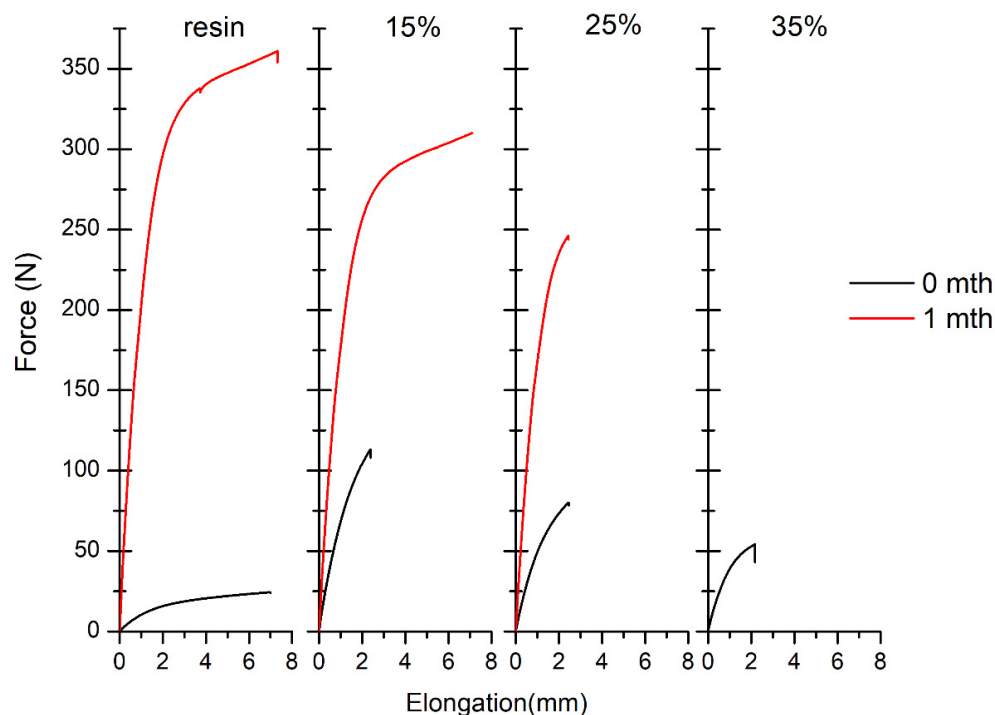


**Figure 3.** The course of representative curves formed in the stretching test of samples.

Fragments of polymer chains in a network with a high molecular weight and an appropriate degree of cross-linking can respond to the external force during deformation by displacement of the chains, which over time is limited by the cross-links. Only when the maximum strain is reached, does the polymer break in tension. Hence, the apparent plastic nature of the polymer deformation for samples without and with 15% alcohol addition. For samples with higher alcohol content, the deformation is elastic in nature and breaking occurs in a brittle manner, which is most likely caused by the low molecular weight and limited degree of cross-linking.

In the final stage of the termination process, the polymer chains diffuse, being close to the active centers of other macroradicals, and terminate the growth of the chains [20], which can be hindered in the presence of excess solvent, so that the formed chains terminate with the radicals derived from the solvent and not with the other macroradicals, limiting the increase in molecular weight and degree of cross-linking. This theory is reflected in the values of relative strain, where for samples with lower alcohol content, an increase in elongation is seen after one month, when the termination took place mainly between the chains of the formed polymer; while for samples with higher solvent content, it is seen that the strain is maintained at the same low level of about 4% even after termination.

Termination by chain transfer does not reduce the number of radicals in the system, causing little or no change in the reaction rate, and thus reducing the final polymerization time compared to solvent-free polymerization, in which the reaction rate decreases due to disproportionation and/or combination [32]. Keeping the sample fabrication parameters

constant, including the exposure time of the layers to UV radiation, may have resulted in negative radiation effects on the structure and properties of the samples with alcohol, for which the polymerization time was most likely shortened. The exact chemical structures of the resin monomers are not known, but their general name is low molecular weight urethane acrylate polymer [22]. In this type of resin without the addition of a suitable photostabilizer, UV exposure has been shown to cause scission of the urethane bond and photodegradation [33], which would ultimately reduce the molecular weight, complementing speculation about the negative effect of the reduced polymer molecular weight on the mechanical parameters. Excessive exposure time may also cause additional reactions related to the presence of radicals in the structure after polymerization, leading to degradation and formation of new resin components, which may have caused the discoloration of the samples seen in Figure 1.

### 3.4. Raman Spectroscopy Characterization

The average Raman spectra of cured pure resin and resin with 15%, 25%, and 35% alcohol content are shown in Figure 4. No additional bands were observed due to the addition of ethanol. The addition of alcohol causes the disappearance of the band located at 1409 cm$^{-1}$ attributed to C=CH$_2$ scissoring deformation vibrations in acrylate resin [34]. This is probably due to the easier diffusion of solvent molecules during the polymerization process than of macroradicals and the effective quenching of active centers by ethanol, which increases the conversion rate by making it more difficult to combine macroradicals into long chains, which correlates with previous considerations. A change in the integral intensity ratio of the bands 1609/1634 cm$^{-1}$, associated with the C=C phenyl vibrations and C=C meth-acrylate stretching vibrations [35] due to the use of ethanol, can be observed. This also confirms the reduction in the proportion of double bonds present in the structure of the resin after curing, which is caused by the cross-linking process.
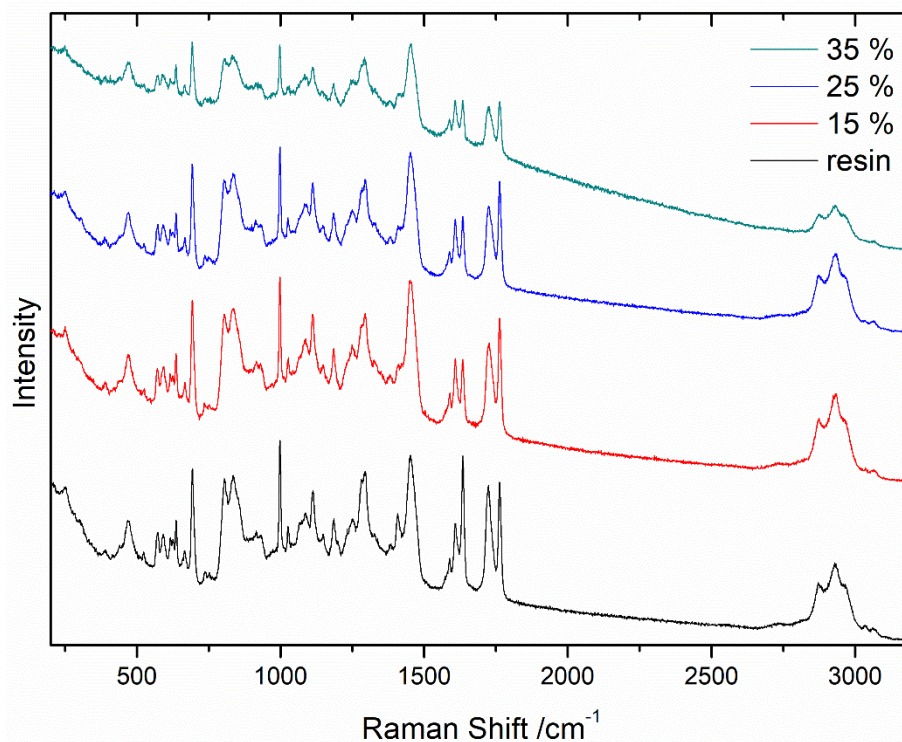


**Figure 4.** The averaged Raman spectra of resin (black), and resin with an alcohol content of 15% (red), 25% (blue), and 35% (green).

## 4. Conclusions

The results demonstrate the significant effect of ethanol on the properties of acrylic-urethane resin. The study justifies the planned use of ethanol as a cosolvent to dissolve agomelatine in resin for transdermal applications, identifying 15% ethanol as the optimal concentration. Higher concentrations of alcohol degrade the material properties, limiting its potential for microneedle transdermal systems. Further research should focus on the photopolymerization process, including the effect of ethanol on radical polymerization rates, molecular weight, and cross-linking. To obtain a resin–15% ethanol solution, 3.5 g of ethanol is required per 20 g of resin, allowing the dissolution of 215.6 mg of agomelatine. This concentration allows for the production of samples containing up to 21.56 mg of agomelatine, which is close to the standard daily dose [36]. Improvements in radical polymerization processes, alternative solvents, or increased sample weights are needed to increase the agomelatine content. Future studies should also optimize drug release efficiency, taking into account the medium, time, and diffusion capabilities influenced by intermolecular interactions between resin and drug.

**Author Contributions:** Conceptualization, D.T., T.O. and R.W.; Data curation, A.B.N.; Formal analysis, D.T.; Funding acquisition, T.O.; Investigation, D.T. and R.W.; Methodology, W.K. and M.S.; Project administration, T.O. and M.S.; Resources, W.K.; Software, W.K.; Validation, M.W.; Visualization, A.B.N.; Writing—original draft, D.T.; Writing—review and editing, D.T., A.B.N., M.W. and R.W. All authors have read and agreed to the published version of the manuscript.

**Data Availability Statement:** Dataset available on request from the authors.

**Conflicts of Interest:** The authors declare that they have no known competing financial interests or personal relationships that could have appeared to influence the work reported in this paper. The authors declare no conflict of interest.

## References

1. Laskowska, D.; Mitura, K.; Ziółkowska, E.; Bałasz, B. Additive manufacturing methods, materials and medical applications–the review. *J. Mech. Energy Eng.* **2021**, *5*, 15–30. [CrossRef]
2. Shirinbayan, M.; Zirak, N.; Benfriha, K.; Farzaneh, S.; Fitoussi, J. *Polymer Materials in Additive Manufacturing: Modelling and Simulation*, 1st ed.; MDPI: Basel, Switzerland, 2023. [CrossRef]
3. Mitchell, A.; Lafont, U.; Hołyńska, M.; Semprimoschnig, C. Additive manufacturing—A review of 4D printing and future applications. *Addit. Manuf.* **2018**, *24*, 606–626. [CrossRef]
4. Quan, H.; Zhang, T.; Xu, H.; Luo, S.; Nie, J.; Zhu, X. Photo-curing 3D printing technique and its challenges. *Bioact. Mater.* **2020**, *5*, 110–115. [CrossRef] [PubMed]
5. Grzegorz, T.G. Review of Additive Manufacturing Methods. *Solid State Phenom.* **2020**, *308*, 1–20. [CrossRef]
6. Lee, H.E.; Alauddin, M.S.; Ghazali, M.I.M.; Said, Z.; Zol, S.M. Effect of Different Vat Polymerization Techniques on Mechanical and Biological Properties of 3D-Printed Denture Base. *Polymers* **2023**, *15*, 1463. [CrossRef] [PubMed]
7. Chaudhary, R.; Fabbri, P.; Leoni, E.; Mazzanti, F.; Akbari, R.; Antonini, C. Additive manufacturing by digital light processing: A review. *Prog. Addit. Manuf.* **2023**, *8*, 331–351. [CrossRef]
8. Zhang, J.; Hu, Q.; Wang, S.; Tao, J.; Gou, M. Digital light processing based three-dimensional printing for medical applications. *Int. J. Bioprint.* **2020**, *6*, 242. [CrossRef] [PubMed]
9. Wang, F.Y.; Chen, Y.; Huang, Y.Y.; Cheng, C.M. Transdermal drug delivery systems for fighting common viral infectious diseases. *Drug Deliv. Transl. Res.* **2021**, *11*, 1498–1508. [CrossRef] [PubMed]
10. Nguyen, T.T.; Park, J.H. Human studies with microneedles for evaluation of their efficacy and safety. *Expert Opin. Drug Deliv.* **2018**, *15*, 235–245. [CrossRef]
11. Turner, J.G.; White, L.R.; Estrela, P.; Leese, H.S. Hydrogel-Forming Microneedles: Current Advancements and Future Trends. *Macromol. Biosci.* **2021**, *21*, e2000307. [CrossRef] [PubMed]
12. Pagac, M.; Hajnys, J.; Ma, Q.P.; Jancar, L.; Jansa, J.; Stefek, P.; Mesicek, J. A review of vat photopolymerization technology: Materials, applications, challenges, and future trends of 3d printing. *Polymers* **2021**, *13*, 598. [CrossRef] [PubMed]
13. Shah, D.M.; Morris, J.; Plaisted, T.A.; Amirkhizi, A.V.; Hansen, C.J. Highly filled resins for DLP-based printing of low density, high modulus materials. *Addit. Manuf.* **2021**, *37*, 101736. [CrossRef]
14. Bragaglia, M.; Paleari, L.; Passaro, J.; Russo, P.; Fabbrocino, F.; Luciano, R.; Nanni, F. 3D printing of biodegradable and self-monitoring SWCNT-loaded biobased resin. *Compos. Sci. Technol.* **2023**, *243*, 110253. [CrossRef]

15. Varghese, G.; Moral, M.; Castro-García, M.; López-López, J.J.; Marín-Rueda, J.R.; Yagüe-Alcaraz, V.; Hernández-Afonso, L.; Ruiz-Morales, J.C.; Canales-Vázquez, J. Fabricación y caracterización de cerámicas medinate impresión 3D DLP de bajo coste. *Bol. Soc. Esp. Ceram. Vidr.* **2018**, *57*, 9–18. [CrossRef]

16. Roumanie, M.; Flassayer, C.; Resch, A.; Cortella, L.; Laucournet, R. Influence of debinding and sintering conditions on the composition and thermal conductivity of copper parts printed from highly loaded photocurable formulations. *SN Appl. Sci.* **2021**, *3*, 55. [CrossRef]

17. Chen, K.Y.; Zeng, J.J.; Lin, G.T. Fabrication of 5-fluorouracil-loaded tablets with hyperbranched polyester by digital light processing 3D printing technology. *Eur. Polym. J.* **2022**, *171*, 111190. [CrossRef]

18. Lim, S.H.; Kathuria, H.; Bin Amir, M.H.; Zhang, X.; Duong, H.T.; Ho, P.C.L.; Kang, L. High resolution photopolymer for 3D printing of personalised microneedle for transdermal delivery of anti-wrinkle small peptide. *J. Control. Release* **2021**, *329*, 907–918. [CrossRef]

19. Nezu, T.; Nagano-Takebe, F.; Endo, K. Designing an antibacterial acrylic resin using the cosolvent method—Effect of ethanol on the optical and mechanical properties of a cold-cure acrylic resin. *Dent. Mater. J.* **2017**, *36*, 662–668. [CrossRef] [PubMed]

20. Yamada, B. Free-Radical Addition Polymerization (Fundamental). In *Encyclopedia of Polymeric Nanomaterials*; Kobayashi, S., Müllen, K., Eds.; Springer: Berlin/Heidelberg, Germany, 2015. [CrossRef]

21. Demyttenaere, K. Agomelatine: A narrative review. *Eur. Neuropsychopharmacol.* **2011**, *21*, S703–S709. [CrossRef] [PubMed]

22. Raydent SG Data Sheet. 2023. Available online: https://esdent.pl/images/instrukcje/RAYDENT-SDS-SG-2.2.pdf (accessed on 4 December 2023).

23. Tomczak, D.; Wichniarek, R.; Kuczko, W.; Górski, F. Manufacturing of thin-walled, complex polymer parts by DLP printing–the influence of process parameters on crosslinking density. *Bull. Pol. Acad. Sci. Tech. Sci.* **2023**, *71*, e145936. [CrossRef]

24. Hamama, H.H. Recent advances in posterior resin composite restorations. In *Applications of Nanocomposite Materials in Dentistry*; Elsevier: Duxford, UK, 2019; pp. 319–336. [CrossRef]

25. Topa-Skwarczyńska, M.; Ortyl, J. Photopolymerization Shrinkage: Strategies for Reduction, Measurement Methods and Future Insights. *Polym. Chem.* **2023**, *14*, 2145–2158. [CrossRef]

26. Magee, C.; Sugihara, Y.; Zetterlund, P.B.; Aldabbagh, F. Chain transfer to solvent in the radical polymerization of structurally diverse acrylamide monomers using straight-chain and branched alcohols as solvents. *Polym. Chem.* **2014**, *5*, 2259–2265. [CrossRef]

27. Basu, S.; Sen, J.N.; Palit, S.R. Degree of polymerization and chain transfer in methyl methacrylate. *Proc. R. Soc. Lond. A Math. Phys. Sci.* **1950**, *202*, 485–498. [CrossRef]

28. Luo, Y.R. *Comprehensive Handbook of Chemical Bond Energies*, 1st ed.; CRC Press: Boca Raton, FL, USA, 2007. [CrossRef]

29. Oliver, J.D.; Gaborieau, M.; Castignolles, P. Ethanol determination using pressure mobilization and free solution capillary electrophoresis by photo-oxidation assisted ultraviolet detection. *J. Chromatogr. A* **2014**, *1348*, 150–157. [CrossRef] [PubMed]

30. Wu, X.; Zhu, C. Recent advances in alkoxy radical-promoted C-C and C-H bond functionalization starting from free alcohols. *Chem. Commun.* **2019**, *55*, 9747–9756. [CrossRef] [PubMed]

31. Slouf, M.; Strachota, B.; Strachota, A.; Gajdosova, V.; Bertschova, V.; Nohava, J. Macro-, micro-and nanomechanical characterization of crosslinked polymers with very broad range of mechanical properties. *Polymers* **2020**, *12*, 2951. [CrossRef] [PubMed]

32. Soroush, M.; Rappe, A.M. Theoretical Insights Into Chain Transfer Reactions of Acrylates. In *Computational Quantum Chemistry: Insights into Polymerization Reactions*, 1st ed.; Soroush, M., Ed.; Elsevier: Amsterdam, The Netherlands, 2019. [CrossRef]

33. Decker, C.; Zahouily, K. Photodegradation and photooxidation of thermoset and UV-cured acrylate polymers. *Polym. Degrad. Stab.* **1999**, *64*, 293–304. [CrossRef]

34. Szybowicz, M.; Nowicka, A.B.; Sądej, M.; Andrzejewska, E.; Drozdowski, M. Morphology of polyacrylate/nanosilica composites as studied by micro-Raman spectroscopy. *J. Mol. Struct.* **2014**, *1070*, 131–136. [CrossRef]

35. Okulus, Z.; Buchwald, T.; Szybowicz, M.; Voelkel, A. Study of new resin-based composites containing hydroxyapatite filler using Raman and infrared spectroscopy. *Mater. Chem. Phys.* **2014**, *145*, 304–312. [CrossRef]

36. Karademir, B. The assessment of effectiveness of a novel antidepressant, Agomelatine on anxiety and depression induced by fluoride intoxication by means of Open-Field and Hot-Plate tests in mouse model (BalB-C). *Ank. Univ. Vet. Fak. Derg.* **2023**, *70*, 123–130. [CrossRef]